Cellulose (2020) 27:4407–4416
https://doi.org/10.1007/s10570-020-03080-2

ORIGINAL RESEARCH

Enhanced mechanical performance of xylan-based composite hydrogel via chain extension and semi-interpenetrating networks

Nan Li · Ya-jie Hu · Jing Bian · Ming-fei Li · Xiang Hao · Feng Peng · Run-Cang Sun

Received: 6 October 2019 / Accepted: 24 February 2020 / Published online: 9 March 2020

Abstract Improving the mechanical performance of hemicellulose-based hydrogel is an enormous challenge. Here, we propose a new strategy to achieve the hemicellulose-based hydrogels with superior mechanical performance through chain extension and semi-interpenetrating polymeric networks (semi-IPN). Xylan, known as the main type of hemicelluloses in angiosperms, is successfully modified to increase molecular weight by reductive amination reaction, overcoming the major limitation of brittleness. Then, the chemical network is obtained by graft copolymerizing acrylic acid (AA) with cross-linking agent *N,N′*-methylenebisacrylamide (MBA) in the presence of chain extended xylan (CEX). With the further introduction of ferric ions, a physical network is constructed via metal–ligand interactions. Such a xylan-based semi-IPN hydrogel shows excellent mechanical properties with a fracture tensile stress of 1.4 MPa, compression stress of 0.59 MPa, and the elongation at break of 1136%. In addition, the hydrogel also exhibits fine water absorbency (213.6 g/g) and high electrical conductivity (4.76×10^{-3} S/m). We anticipate that the resultant xylan-based semi-IPN hydrogels will open up a new approach for the design of high performance hemicellulose-based soft materials.

Keywords Chain extended xylan · Semi-IPN · Mechanical performance · Water absorbency

Electronic supplementary material The online version of this article (https://doi.org/10.1007/s10570-020-03080-2) contains supplementary material, which is available to authorized users.

N. Li · Y. Hu · J. Bian · M. Li · X. Hao · F. Peng (✉)
Beijing Key Laboratory of Lignocellulosic Chemistry, Beijing Forestry University, Beijing 100083, China
e-mail: fengpeng@bjfu.edu.cn

F. Peng
Beijing Advanced Innovation Center for Tree Breeding by Molecular Design, Beijing Forestry University, Beijing 100083, China

R.-C. Sun
Center for Lignocellulose Science and Engineering, Dalian Polytechnic University, Dalian 116034, China

Introduction

Hydrogels are three-dimensional cross-linked hydrophilic polymer networks with strong water absorption ability. In general, they are soft and wet, with poor mechanical performance. Given the ever-increasing need to apply hydrogels in various fields, several strategies have been developed to increase the mechanical performance of hydrogels, including the introduction of semi-IPN structure (Gong et al. 2003), the development of topological sliding rings (Okumura and Ito 2001; Ito 2007, 2010), the fabrication of conjoined-network (Fei et al. 2013; Xu et al. 2019), the construction of mechanoresponsive chains (Ramirez et al. 2013), etc. These tough hydrogels have been applied for

biomedicine actuators (Haraguchi and Li 2005; Huang et al. 2007; Tang et al. 2010) and machines (Tanabe et al. 2008; Yasuda et al. 2005, 2009; Shin et al. 2012), owing to their excellent mechanical performance. Most of them are composed of synthetic polymers, which need considerable resources for synthesis and lack of biodegradability. It thus would be intriguing to develop biopolymer-based hydrogels with outstanding mechanical performance since they are abundantly available and biodegradability.

Hemicelluloses, as the second most abundant renewable natural polymer, account for 20–35% of lignocellulosic biomass (Peng et al. 2010). Much attention has been paid to the development and application of hemicelluloses-based products. Xylan, the main type of hemicellulose as well as the major non-cellulosic polysaccharide in angiosperms, has a typical structure with $\beta-(1\rightarrow 4)$ linked D-xylose as the backbone, and 4-*O*-methyl-D-glucuronopyranosyl or D-glucuronopyranosyl substituents at C-2 and/or C-3 as the side chains (Yin et al. 2013). Hydroxyl groups are useful functional groups in xylan (Imran et al. 2013), whereby great efforts have been made by chemical modification of hydroxyl groups (Stuart et al. 2010; Wilkie 1979). Xylan-type hemicelluloses are considered as the suitable raw materials to prepare hydrogels, which have potential applications in biomedical fields (Cao et al. 2014). For example, xylan-based hydrogels are beneficial as controllable release carriers in the human digestive system (Peng et al. 2012). The injectability and temperature response of xylan/chitosan hybrid hydrogel make it suitable for the use of bone tissue regeneration (Yang et al. 2011). Xylan-based temperature/pH sensitive hydrogels are also designed for controlled drug release (Zhao et al. 2014). Specifically, the xylan-based hydrogels are prepared by the cross-linking polymerization of xylan with *n*-isopropylacrylamide (NIPAm) and acrylic acid (AA) under UV irradiation (Liu et al. 2018). This type of hydrogel is further exploited for the release of acetylsalicylic acid, with the cumulative release rate approaching to 90.5% in 5 h. Therefore, xylan-based hydrogels should be gaining increased relevance in material science. In fact, compared to the commercially available polysaccharides such as cellulose (Sahiner and Demirci 2017) or starch (Heidarian et al. 2017), the industrial application of xylan is still less due to the poor mechanical performance resulting from its low molecular weight.

Aside from the mechanical performance, biohydrogels possessing other properties including water absorbency and electrical conductivity will be appealing. Generally, ionic bonding or coordinate cross-linking has been utilized as an additional mean to endow the biohydrogels with multi-functions. Much effort has been made to introduce metal ion complexes into the 3D network of biohydrogels (Li and Pan 2010). In previous works, the tough multifunctional hydrogels containing different metal ions have been prepared, such as alginate-Ca^{2+} hydrogel (Ebringerová et al. 2002) and chitosan-Mn^{2+} hydrogel (Bush et al. 2006). In addition, the ion interactions in the hydrogel materials are less sensitive to the moisture than hydrogen bonds, which further extend the practical applications of biohydrogel. However, there are very few reports on the xylan-metal ions based tough multifunctional hydrogels.

In this work, we presented a facile route to develop tough xylan-based hydrogels with good water absorbency and high electrical conductivity. Xylan was initially modified via reductive amination to synthesize CEX with increased chain length and molecular weight. Monomer AA and the cross-linker MBA were then graft copolymerized in the presence of CEX to prepare the chemical cross-linked network. Further, the metal ions Fe^{3+} were incorporated to build the network by ionic coordination between Fe^{3+} and $-COO^{-}$ groups. The physical and chemical properties of hydrogels were characterized by Fourier-transform infrared spectroscopy (FT–IR), scanning electron microscopy (SEM), and differential scanning calorimeter (DSC). In addition, the mechanical property and swelling ability of hydrogels were also investigated. The prepared hydrogels showed excellent mechanical properties as well as tunable water adsorption and conductivity, making them promising candidates in the fields of electronic skin, sensor, degradable material, and tissue engineering.

Materials and methods

Materials

The xylan was extracted from bamboo (*Phyllostachys pubescens*) holocelluloses by the alkaline extraction method (Guan et al. 2014). The sugar compositions of xylan were 83.5% xylose, 5.1% arabinose, 4.2%

glucose, 0.4% galactose, and 6.8% glucuronic acid (relatively molar percent). The xylan had a weight average molecular-weight (M_w) of 13,400 g mol^{-1} and a polydispersity of 4.1, which was determined by gel permeation chromatography (GPC) (Peng et al. 2009). Sodium cyanoborohydride ($NaBH_3CN$, 95%) was purchased from Beijing Bailingwei Co., Ltd. 1,2-Ethylenediamine (≥ 99.5%) was purchased from Tianjin FuChen Chemical Reagent Factory. Ammonium persulphate (APS) was purchased from Xilong Chemical Co., Ltd. Acrylic acid (AA) and ethanol were purchased from Beijing Chemical Works. *N,N,N',N'*-Tetra-methylethylenediamine (TEMED) was obtained from AMRESCO. *N,N'*-Methylene-bis-acrylamide (MBA) was purchased from Chengdu Gray West Chemistry Technology Co., Ltd. All the reagents mentioned above were directly used without further purification.

Methods

Chain extension reaction of xylan

Chain extending reaction of xylan was conducted via a two-step reductive amination process (Edlund and Albertsson 2012), as illustrated in Fig. 1. The xylan (3.0 g) was dissolved in 20 mL deionized water, and then 1,2-ethylenediamine (0.34 g) was added. Thereafter, the pH was adjusted to 6.0 using 1.0 mol/L HCl solution, and $NaBH_3CN$ (0.188 g) was added. After the reaction was carried out for 24 h at room temperature, amine-modified xylan denoted as AMX was recovered by ethanol precipitation. AMX was washed three times with ethanol and dried under reduced pressure at room temperature. In the following section, AMX (1.0 g) and xylan (1.0 g) were dissolved in 20 mL deionized water, and $NaBH_3CN$ (0.115 g) was added. The reaction mixture was stirred at room temperature for 24 h, and the product denoted CEX was recovered by ethanol precipitation. The obtained CEX was then washed three times with ethanol and dried under reduced pressure at room temperature.

Preparation of xylan-based hydrogels

CEX (0.1 g) were firstly dissolved in 10 mL of distilled water with mechanical stirring at 60 °C for 1 h, then the solution was cooled to room temperature. 0.05 g of APS and 0.05 mL of TEMED as an initiator system were added into the CEX solution, and the mixture was stirred for 10 min to generate the free radicals. After variable amounts of AA (0.8–1.6 g), cross-linking agent MBA (0.005–0.025 g), and $FeCl_3 \cdot 6H_2O$ (0.1–1.0%) was added, the mixture solution continued to be stirred at ambient temperature for 2 h. After that, the mixture solution was transferred into a centrifuge tube (10 mL), and the cross-linking reaction was allowed to proceed at 65 °C for 24 h without mechanical stirring. Finally, the hydrogels were carefully removed from the centrifuge tubes to test the properties. Figure 1 showed the synthetic mechanism of hydrogels. The compositions of the fabricated hydrogels are shown in Table 1.

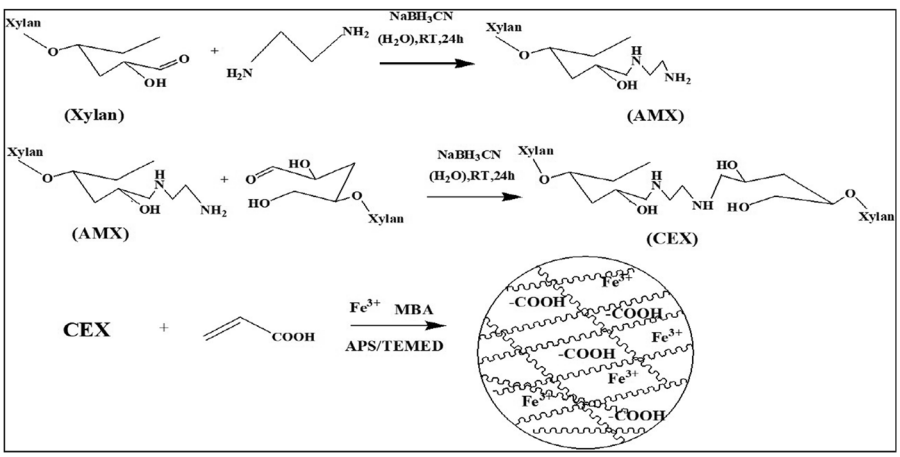

Fig. 1 The synthetic process of AMX, CEX, and composite hydrogels

FT–IR spectroscopy

FT–IR spectra of the hydrogels were recorded using a Thermo Scientific Nicolet in 10 FT-IR microscope (Thermo Nicolet Corporation, Madison, WI), the spectra were recorded from 4000 to 400 cm^{-1} at resolution of 4 cm^{-1} and 128 scans.

Morphology of hydrogels

The sectional structures of the composite hydrogels were measured by scanning electron microscopy (SEM) (HitachiS-3400NII) to observe the internal micro-structure.

Thermal analysis

Thermal analysis was performed by differential scanning calorimeter (DSC) on a simultaneous thermal analyzer (PYRIS Diamond TG; PerkinElmer Instruments). The apparatus was continually flushed with nitrogen. A sample weighing between 30 and 50 mg was heated from room temperature to 600 °C at the heating rate of 10 °C/min.

Mechanical test

Mechanical properties of hydrogels were examined using an electronic universal testing machine (Zwick/roell) with a load cell of 100 N at room temperature. The tensile tests of the cylindrical sample (100 mm length and 2 mm diameter) were stretched at a crosshead speed of 60 mm min^{-1}. The compression tests of the cylindrical sample (30 mm height and 20 mm diameter) were conducted at a crosshead speed of 10 mm min^{-1}. The elastic modulus of hydrogels was determined from the gradient of the stress–strain curves. The ten samples were tested (Table 1).

Swelling capacity

The freeze–dried composite hydrogels (m_0) were weighed and then immersed into distilled water to test their swelling capacity at room temperature. The weight gain of the samples was monitored gravimetrically. The mass of the wet hydrogels (m_{eq}) was determined after removal of the surface water by gently dabbing the hydrogels with filter paper. The equilibrium swelling ratio (Q_{eq}) was determined by the equation:

$$Q_{eq} = \left(m_{eq} - m_0\right)/m_0 \quad (1)$$

where m_0 and m_{eq} are the masses of the freeze-dried hydrogel and the swollen hydrogel, respectively (Hansen and Plackett 2008).

The electrical conductivity measurement and behavior of hydrogels

The electrical conductivity (σ) of hydrogels were measured by a Source Meter (ST-2258C, Suzhou) containing a digital four-probe tester with a linear probe head (2.0 mm space) after freeze-dried 48 h via (7387071 LABCONCO 4.5L Freeze Dry System). The electrical conductivity was calculated using the following equation reported in literature:

$$\sigma = \frac{1}{\rho} \quad (2)$$

where ρ represent the resistance of the hydrogels.

Table 1 Compositions of the fabricated hydrogels

Samples	CEX (g)	APS (g)	TEMED (mL)	Fe^{3+} (%)	MBA (g)	AA (g)
$AA_{0.8}$	0.1	0.05	0.05	0.5	0.010	0.8
$AA_{1.2}$	0.1	0.05	0.05	0.5	0.010	1.2
$AA_{1.6}$	0.1	0.05	0.05	0.5	0.010	1.6
$M_{0.005}$	0.1	0.05	0.05	0.5	0.005	0.8
$M_{0.015}$	0.1	0.05	0.05	0.5	0.015	0.8
$M_{0.020}$	0.1	0.05	0.05	0.5	0.020	0.8
$Fe^{3+}{}_{0.1}$	0.1	0.05	0.05	0.1	0.010	0.8
$Fe^{3+}{}_{0.3}$	0.1	0.05	0.05	0.3	0.010	0.8
$Fe^{3+}{}_{0.7}$	0.1	0.05	0.05	0.7	0.010	0.8
$Fe^{3+}{}_{1.0}$	0.1	0.05	0.05	1.0	0.010	0.8

Results and discussion

Design rationale of the xylan-based semi-IPN hydrogel.

The tough hydrogel derived from xylan was designed by the combination of chain extended reaction of xylan and semi-IPN structure. The chain-extended xylan (CEX) was prepared by reductive amination of xylan with 1,2-ethylenediamine as reducing amination coupling agent (Fig. 1). In the first step, amine-modified xylan (AMX), as the important intermediary, was prepared by reacting xylan with an excess of 1,2-ethylenediamine, which was subsequently reduced to a more stable secondary amine with sodium cyanoborohydride ($NaBH_3CN$) as reducing agent. Notably, $NaBH_3CN$ was a weak reducing agent that could selectively react with imine groups of AMX in the presence of a wide variety of other functional groups, such as carbonyl, carboxyl, and unsaturated structures (Turhan et al 2013). In the second step, the resulting amine-terminated xylan chains were then coupled with a nearly equivalent amount of xylan reducing-end aldehydes via a reductive amination procedure, as it was with the first step.

The composite hydrogels were prepared based on the chain-extended xylan (CEX) and AA by free radical graft co-polymerization in the presence of cross-linking agent *N,N′*-methylenebisacrylamide (MBA). Briefly, sulfate anion radical generated from the heated APS can extract hydrogen atom from the hydroxyl group of xylan, thus forming alkoxy radicals, resulting in active centers of xylan, and subsequently initiating the polymerization radically. The cross-linker (MBA) in the system led to the formation of the first chemical crosslinked co-polymer network, preventing the dissolution of the hydrophilic polymer. In order to enhance the mechanical properties of hydrogels, ferric ions (Fe^{3+}) were added into the hydrogel to form the physically cross-linked network via metal–ligand interactions. The compositions of the resulted hydrogel were illustrated in Table 1.

Structure study of hydrogel

FT–IR analysis was carried out to verify the occurrence of graft polymerization and semi-IPN structure of CEX-*g*-PAA/Fe^{3+}. As shown in Fig. 2, for the xylan, the strong broad absorption peak at 3420 cm^{-1} was attributed to the stretching vibration of –OH, and the band at 2910 cm^{-1} was attributed to symmetric vibration of C–H, while the prominent absorption peak at 1040 cm^{-1} was originated from the C–O–C stretching vibration (Peng et al. 2009). As for the AMX, the band at 1260 cm^{-1} was due to the stretching vibration of C–N in 1,2-ethylenediamine. However, it disappeared in the spectrum of CEX, suggesting a successful coupling reaction between unmodified xylan and amine-terminated xylan (Anas et al. 2015). In terms of the semi-IPN structure of CEX-*g*-PAA/Fe^{3+} sample, the decreased intensity of peak at 3420 cm^{-1} was ascribed to the –OH deformation in free radical reaction, and the band at 1720 cm^{-1} in the hydrogel was ascribed to C = O stretching corresponding to $–COO^-$ from PAA. Furthermore, the changes in the fingerprint region (840–576 cm^{-1}) were attributed to the Fe^{3+}–O vibration, implying the formation of metal oxygen bond (Hussain et al. 2018). We reasoned that AA monomers were grafted onto the backbone of CEX in the presence of MBA, and semi-IPN hydrogels were prepared successfully.

SEM experiments were conducted to gain insight into the inner network structure. From Fig. 3a–d, all hydrogels showed different degrees of wrinkles or pores on their surfaces, which may be ascribed to the different cross-linking density of gel structures. Figure 3a exhibited the distinct CEX-*g*-PAA hydrogel

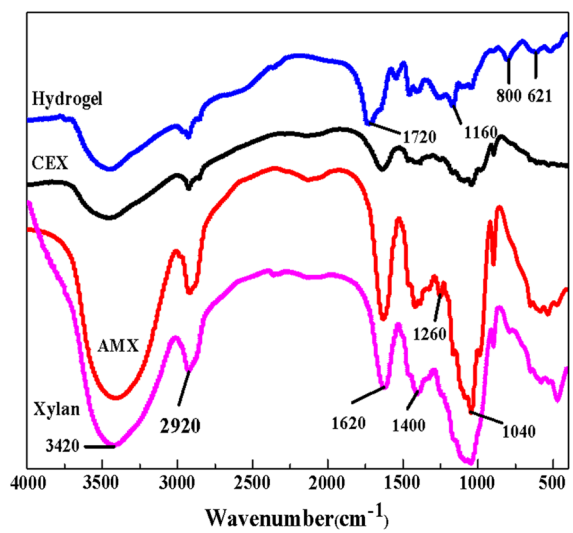

Fig. 2 FT-IR spectra of xylan, AMX, CEX and CEX-*g*-PAA/Fe^{3+} hydrogels

morphology with spongy surfaces and several interspatial voids. These folds not only expanded the specific surface area of the hydrogel, but also improved the swelling capacity. In terms of the CEX-*g*-PAA/Fe^{3+} semi-IPN hydrogel, the addition of Fe^{3+} led to lots of regular and large pores on the sample surface (Fig. 3b). Moreover, the amount and diameter of pores decreased gradually with the Fe^{3+} concentration increased from 0.1 to 0.7% (Fig. 3c and d). It thus could be concluded that the higher concentration of Fe^{3+} would cause the larger cross-linking density, leading to the formation of more stable and much denser hydrogels network structure.

The DSC thermograms of the CEX-*g*-PAA hydrogel and CEX-*g*-PAA/Fe^{3+} hydrogel further revealed the influences of structure discrepancy on thermal stability. In Fig. 3e, the subtle endothermic peak in the range of 50–90 °C represented the typical water loss (Xiao et al. 2016). The exothermic peak appeared at 256 °C was ascribed to the decomposition of xylan, which reported in the relevant literature (Azizullah et al. 2016). Generally, the fragmentation of hydrogel framework was degraded into small molecules at 456–600 °C (Aziz and Ansell 2004). The CEX-*g*-PAA hydrogel sample showed two endothermic peaks at 450 °C and 496 °C, which were corresponded to the degradation of the CEX-*g*-PAA hydrogel. In the case of CEX-*g*-PAA/Fe^{3+} hydrogel, the second endothermic peak at 496 °C was shifted to 577 °C owing to the presence of semi-IPN structure, consistent with the idea that the CEX-*g*-PAA/Fe^{3+} hydrogel was more stable than the CEX-*g*-PAA hydrogel.

Mechanical performance study

As can be seen from Fig. 4a–c, it was difficult to stand by tiny compression for the typical xylan-based hydrogels. By comparison, the CEX-*g*-PAA and CEX-*g*-PAA/Fe^{3+} samples exhibited much better mechanical performance than the xylan-based hydrogel. In view of the poor mechanical performance of typical xylan-based hydrogels, we wonder if the xylan-based semi-IPN hydrogel was essentially different from the conventional one. As can be seen from Fig. 4d, the compression stress of hydrogels increased slightly with the increased concentration of AA, and all the hydrogel samples showed analogous curves. Besides, both Fig. 4e, f revealed similar Fe^{3+} concentration dependent behavior of the compression stress and strain, which could be attributed to the increase in the degree of entanglement among the chains or cross-linking density. Meanwhile, the dynamic ionic bonds could also serve as sacrificial bonds to dissipate the energy of the hydrogel network, thus improving the mechanical properties. Furthermore, the maximum strain and stress were 136% and

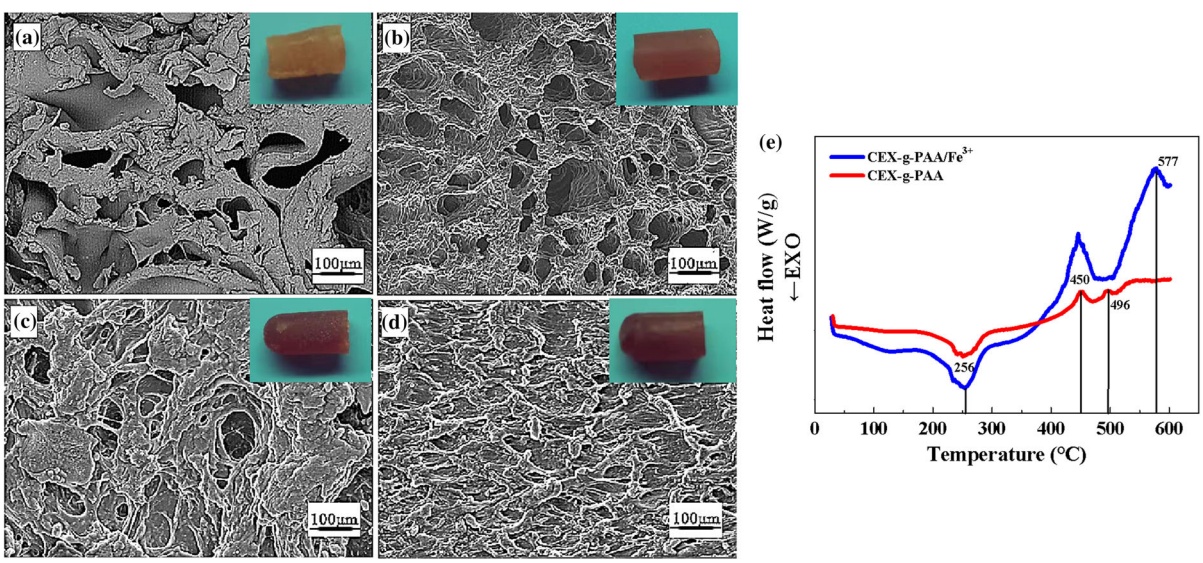

Fig. 3 SEM images of hydrogels: **a** CEX-*g*-PAA; **b** CEX-*g*-PAA/$Fe^{3+}{}_{0.1}$; **c** CEX-*g*-PAA/$Fe^{3+}{}_{0.7}$; **d** CEX-*g*-PAA/$Fe^{3+}{}_{1.0}$. **e** The DSC curves of the CEX-*g*-PAA and CEX-*g*-PAA/Fe^{3+} hydrogel, respectively

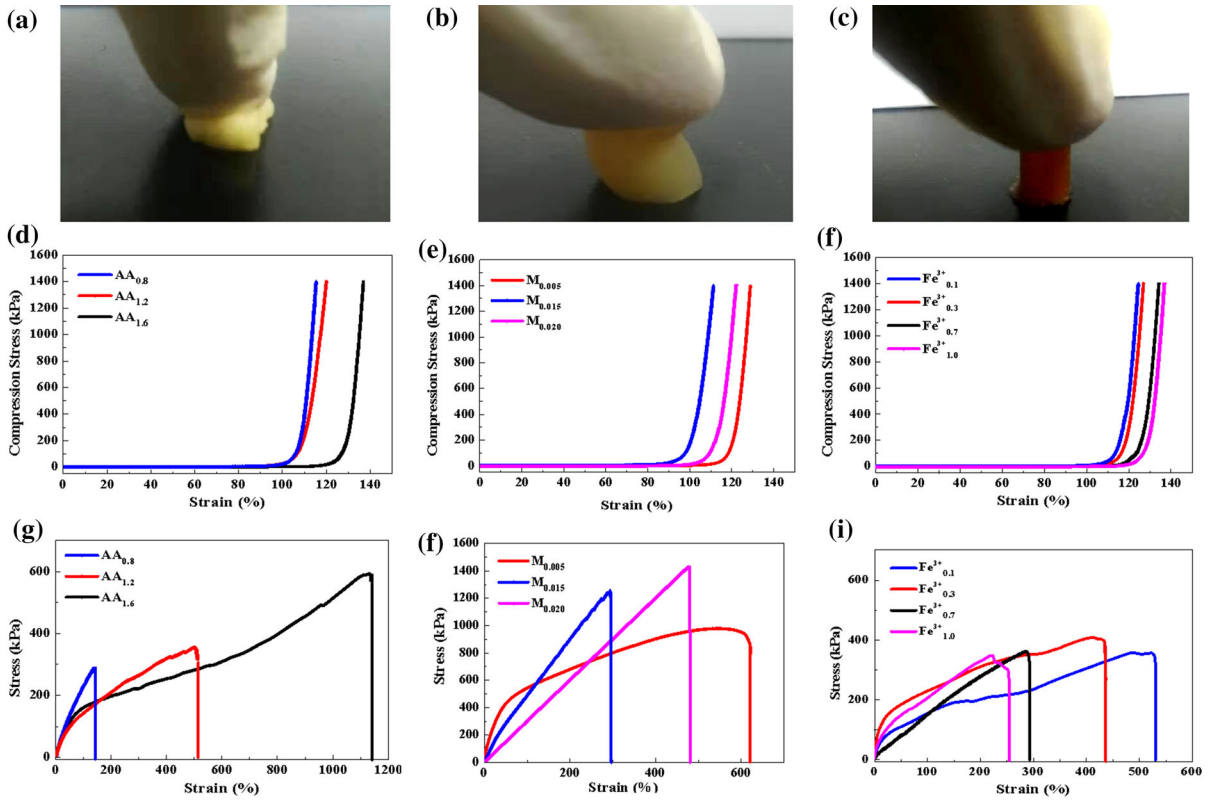

Fig. 4 The photographs of hydrogel samples **a** the compression behavior of sample xylan-*g*-PAA hydrogel; **b** CEX-*g*-PAA hydrogel; **c** CEX-*g*-PAA/Fe^{3+} hydrogel; **d** compression stress–strain curves of hydrogels with different AA concentrations; **e** with different MBA concentrations; and **f** with different Fe^{3+} concentrations; tensile stress–strain curves of hydrogels **g** with different AA concentrations; **h** with different MBA concentrations; **i** with different Fe^{3+} concentrations

1.4 MPa, respectively. It should be noted that most of the hydrogels derived from xylan presented poor mechanical performance, exhibiting much smaller compressive stress (∼ kPa) (Gao et al. 2015). By comparison, the synergic effect of dynamic ion cross-linking and chemical cross-linking in the xylan-based semi-IPN hydrogel contributed to the excellent and remarkable compression properties.

The tensile mechanical properties of the composite hydrogels were further investigated. As illustrated in Fig. 4g, the amount of monomer AA had a considerable positive effect on the tensile mechanical properties of the hydrogels. Rising the AA concentration from 0.8 to 1.6 g would result in the increase of both tensile strength (from 0.14 to 0.36 MPa) and tensile stress at break (from 279 to 1136%). Similarly, the tensile strength increased from 0.94 to 1.25 MPa with an increasing concentration of MBA from 0.005 to 0.015 g, as shown in Fig. 4h. In view of the fact that the cross-linking density became larger with the increase of cross-linking agents, the strength of the hydrogel network was improved accordingly. However, when the concentration of MBA was further increased from 0.015 to 0.020 g, the strain decreased from 621 to 294%. We believed that as the cross-linking points increased, it was difficult to maintain the strain of hydrogels because of the higher density of the gel network structure. Further, all the hydrogel samples with different Fe^{3+} concentrations exhibited excellent flexibility with elongation of more than 250% (Fig. 4i). The elongation decreased with the increased concentration of Fe^{3+}, which was ascribed to the larger number of ionic coordination (Fig. 1), accompanying with the increase of cross-linking density. Notably, when Fe^{3+} concentration was larger than 0.3 mol%, a decline in mechanical properties was observed since the increased cross-linking density would give rise to the decrease of elasticity. In a word,

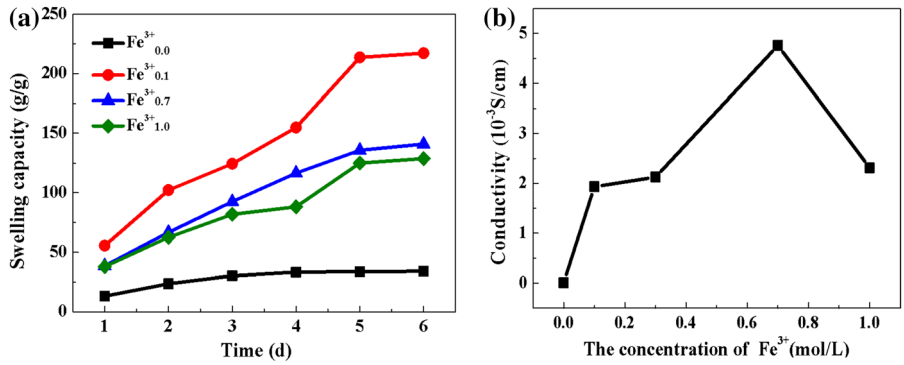

Fig. 5 **a** Swelling kinetic curves of CEX-*g*-PAA/Fe^{3+} hydrogels in distilled water; **b** the conductivity of different Fe^{3+} concentration hydrogels

the xylan-based semi-IPN hydrogels exhibited much better mechanical performance.

Water adsorption and electrical conductivity study

Having established the superior mechanical performance of xylan-based semi-IPN hydrogel, we next investigated the additional property of our hydrogel. In order to study the water absorption behavior, the prepared hydrogel samples ($Fe^{3+}_{0.1}$, $Fe^{3+}_{0.3}$, $Fe^{3+}_{0.7}$, and $Fe^{3+}_{0.0}$) swollen in distilled water for 6 days, and the results were presented in Fig. 5a. With the increase of swelling time, the swelling capacity of all hydrogel samples increased. Importantly, the higher water content could improve the elasticity of hydrogels (Qi et al. 2015). The hydrogel sample ($Fe^{3+}_{0.1}$) had a higher swelling ratio ($\sim$ 213.62 g/g), which was attributed to the relatively loose network structure. As the Fe^{3+} concentration increased from 0.1 to 1.0%, the swelling ratio of hydrogel decreased to 33.67%, which arose from the much denser of the polymer chains. These results are in good agreement with the results of SEM and the mechanical properties.

Metal ions play a key role in the electromagnetic properties of hydrogels, thus we carried out electrical conductivity study. As shown in Fig. 5b, the electrical conductivity of CEX-*g*-PAA hydrogels without Fe^{3+} was about 0.01×10^{-3} S/m. When the mass ratio of Fe^{3+} in the hydrogel rose from 0.1 to 0.7%, the electrical conductivity of the xylan-based semi-IPN hydrogel increased from 1.93×10^{-3} to 4.76×10^{-3} S/m. Under such a circumstance, hydrogels became more conductive owing to the presence of a large number of freely moving ions. With further addition of Fe^{3+} to 1.0%, electrical conductivity dropped to 2.1×10^{-3} S/m unexpectedly. As is known to all, ionic conduction referred to the directional movement of positive and negative ions in the electric field. However, with the addition of excess Fe^{3+}, the positive ions repelled each other, extended the molecular chains and made the dynamic metal ions coordination unstable, resulting in the decrease of electrical conductivity.

Conclusions

In summary, we successfully prepared xylan-based hydrogels featuring excellent mechanical performance, fine water adsorption, and tunable electrical conductivity. By achieving the chain extension, a high molecular weight xylan can be engineered, allowing it to be suitable for the construction of hydrogels. The introduction of semi-IPN further increased the mechanical performance of xylan-based hydrogels, as well as the electrical conductivity. The resultant xylan-based semi-IPN hydrogels can achieve a fracture tensile stress of 1.4 MPa, compression stress of 0.59 MPa, and the elongation at break of 1136%, which was superior to the most existing hemicellulose-based hydrogels. In addition, the water adsorption and electrical conductivity could be easily adjusted by changing the molar fraction of metal ions. This work offers an alternative way to fabricate high-performance xylan-based hydrogels with vast application prospects.

Acknowledgments This research was funded by the Fundamental Research Funds for the Central Universities (BLX201918), Beijing Forestry University Outstanding Young Talent Cultivation Project (2019JQ03017), and National Natural Science Foundation of China (31971611).

Compliance with ethical standards

Conflict of interest All the authors declare that there are no conflicts of interest.

References

Anas IY, Ulrica E, Ann CA (2015) Enhanced formability and mechanical performance of wood hydrolysate films through reductive amination chain extension. Carbohyd Polym 117:346–354

Aziz SH, Ansell MP (2004) The effect of alkalization and fibre alignment on the mechanical and thermal properties of kenaf and hemp bast fibre composites: part 1-polyester resin matrix. Compos Sci Technol 64:1219–1230

Azizullah N-u-R, Liu W, Haider A, Kortz U, Sohail M, Joshi SA, Iqbal J (2016) Novel gelatin-polyoxometalate based self-assembled pH responsive hydrogels: formulation and in vitro characterization. Des Monomers Polym 19:697–705

Bush JR, Liang H, Dickinson M, Botchwey EA (2006) Xylan hemicellulose improves chitosan hydrogel for bone tissue regeneration. Polym Adv Technol 27:1050–1055

Cao XF, Peng XW, Zhong LX, Sun RC (2014) Multiresponsive hydrogels based on xylan-type hemicelluloses and photoisomerized azobenzene copolymer as drug delivery carrier. J Agric Food Chem 62:10000–10007

Ebringerová A, Kardosová A, Hromádková Z, Malovíková A, Hríbalová V (2002) Immunomodulatory activity of acidic xylans in relation to their structural and molecular properties. Int J Biol Macromol 30:1–6

Edlund U, Albertsson AC (2012) SET-LRP goes green: various hemicellulose initiating systems under non-inert conditions. J Polym Sci Part A-Polym Chem 50:2650–2658

Fei RC, George JT, Park J, Means AK, Grunlan MA (2013) Ultra-strong thermoresponsive double network hydrogels. Soft Matter 9:2912–2919

Gao CD, Ren JL, Kong W, Sun RC, Chen Q (2015) Comparative study on temperature/pH sensitive xylan-based hydrogels: their properties and drug controlled release. RSC Advances 5:90671–90681

Gong JP, Katsuyama Y, Kurokawa T, Osada T (2003) Double-network hydrogels with extremely high mechanical strength. Adv Mater 15:1155–1158

Guan Y, Zhang B, Bian J, Peng F, Sun RC (2014) Nanoreinforced hemicellulose-based hydrogels prepared by freeze–thaw treatment. Cellulose 21:1709–1721

Hansen NML, Plackett D (2008) Sustainable films and coatings from hemicelluloses: a review. Biomacromol 9:1493–1505

Haraguchi K, Li HJ (2005) Control of the coil-to-globule transition and ultrahigh mechanical properties of PNIPA in nanocomposite hydrogels. Angew Chem Int Ed 44:6500–6504

Heidarian P, Behzad T, Sadeghi M (2017) Investigation of cross-linked PVA/starch biocomposites reinforced by cellulose nanofibrils isolated from aspen wood sawdust. Cellulose 8:3323–3339

Huang T, Xu H, Jiao K, Zhu L, Brown HR, Wang H (2007) A novel hydrogel with high mechanical strength: a macromolecular microsphere composite hydrogel. Adv Mater 19:1622–1626

Hussain I, Sayed SM, Liu S, Oderinde O, Yao F, Fu G (2018) Glycogen-based self-healing hydrogels with ultra-stretchable, flexible, and enhanced mechanical properties via sacrificial bond interactions. Int J Biol Macromol 117:648–658

Imran AB, Seki T, Takeoka Y (2010) Recent advances in hydrogels in terms of fast stimuli responsiveness and superior mechanical performance. Polym J 42:839–851

Ito K (2007) Novel cross-linking concept of polymer network: synthesis, structure, and properties of slide-ring gels with freely movable junctions. Polym J 39:489–499

Ito K (2010) Slide-ring materials using topological supramolecular architecture. Curr Opin Solid State Mater Sci 14:28–34

Liu XX, Lin QX, Yan YH, Peng F, Sun RC, Ren JL (2018) Hemicellulose from plant biomass in medical and pharmaceutical application: a critical review. Curr Med Chem 24:1–21

Li XM, Pan XJ (2010) Hydrogels based on hemicellulose and lignin from lignocellulose biorefinery: a mini-review. J Biobased Mater Bioenerg 4:289–297

Okumura Y, Ito K (2001) The polyrotaxane gel: a topological gel by figure-of-eight cross-links. Adv Mater 13:485–487

Peng F, Ren JL, Xu F, Bian J, Peng P, Sun RC (2009) Comparative study of hemicelluloses obtained by graded ethanol precipitation from sugarcane bagasse. J Agric Food Chem 57:6305–6317

Peng F, Ren JL, Xu F, Bian J, Peng P, Sun RC (2010) Fractional study of alkali-soluble hemicelluloses obtained by graded ethanol precipitation from sugar cane bagasse. J Agric Food Chem 58:1768–1776

Peng XW, Zhong LX, Ren JL, Sun RC (2012) Highly effective adsorption of heavy metal ions from aqueous solutions by macroporous xylan-rich hemicelluloses-based hydrogel. J Agric Food Chem 60:3909–3916

Qi XM, Guan Y, Chen GG, Zhang B, Ren JL, Peng F, Sun RC (2015) A non-covalent strategy for montmorillonite/xylose self-healing hydrogels. RSC Adv 5:41006–41012

Ramirez ALB, Kean ZS, Orlicki JA, Champhekar M, Elsakr SM, Krause WE, Craig SL (2013) Mechanochemical strengthening of a synthetic polymer in response to typically destructive shear forces. Nat Chem 5:757–761

Sahiner N, Demirci S (2017) Improved mechanical strength of p(AAm) interpenetrating hydrogel network due to microgranular cellulose embedding. J Appl Polym Sci 21:44854–44860

Shin H, Olsen BD, Khademhosseini A (2012) The mechanical properties and cytotoxicity of cell-laden double-network hydrogels based on photocrosslinkable gelatin and gellan gum biomacromolecules. Biomaterials 33:3143–3152

Stuart MAC, Huck WTS, Genzer J, Müller M, Ober C, Stamm M, Sukhorukov GB, Szleifer I, Tsukruk VV, Urban M, Winnik F, Zauscher F, Luzinov I, Minko S (2010) Emerging applications of stimuli-responsive polymer materials. Nat Mater 9:101–113

Tanabe Y, Yasuda K, Azuma C, Taniguro H, Onodera S, Suzuki A, Chen YM, Gong JP, Osada Y (2008) Biological responses of novel high-toughness double network hydrogels in muscle and the subcutaneous tissues. J Mater Sci-Mater Med 19:1379–1387

Tang L, Liu WG, Liu GP (2010) High-strength hydrogels with integrated functions of H-bonding and thermoresponsive surface-mediated reverse transfection and cell detachment. Adv Mater 22:2652–2656

Turhan T, Güvenilir YA, Sahiner N (2013) Micro poly(3-sulfopropyl methacrylate) hydrogel synthesis for in situ metal nanoparticle preparation and hydrogen generation from hydrolysis of $NaBH_4$. Energy 55:511–518

Wilkie KCB (1979) The hemicelluloses of grasses and cereals gramineae. Adv Carbohydr Chem Biochem 36:215–264

Xiao H, Lu W, Le X, Ma C, Li Z, Zheng J, Zhang J, Huang Y, Chen T (2016) A multi-responsive hydrogel with a triple shape memory effect based on reversible switches. Chem Commun 52:13292–13295

Xu L, Wang C, Cui Y, Li A, Qiao Y, Qiu D (2019) Conjoined-network rendered stiff and tough hydrogels from biogenic molecules. Sci Adv 5:34–42

Yang JY, Zhou XS, Fang J (2011) Synthesis and characterization of temperature sensitive hemicellulose-based hydrogels. Carbohyd Polym 86:1113–1117

Yasuda K, Kitamura N, Gong JP, Arakaki K, Kwon HJ, Onodera S, Chen YM, Kurokawa T, Kanaya F, Ohmiya Y, Osada Y (2009) A novel double-network hydrogel induces spontaneous articular cartilage regeneration in vivo in a large osteochondral defect. Macromol Biosci 9:307–316

Yasuda K, Gong JP, Katsuyama Y, Nakayama A, Tanabe Y, Kondo E, Ueno M, Osada Y (2005) Biomechanical properties of high-toughness double network hydrogels. Biomaterials 26:4468–4475

Yin H, Akasaki T, Sun TL, Nakajima T, Kurokawa T, Nonoyama T, Taira T, Saruwatari Y, Gong JP (2013) Double network hydrogels from polyzwitterions: high mechanical strength and excellent anti-biofouling properties. J Mater Chem B 1:3685–3693

Zhao W, Glavas L, Odelius K, Edlund U, Albertsson CA (2014) Facile and green approach towards electrically conductive hemicellulose hydrogels with tunable conductivity and swelling behavior. Chem Mater 26:4265–4273